African Journal of Advanced Pure and Applied Sciences (AJAPAS)
Online ISSN: 2957-644X
Volume 4, Issue 4, 2025
Page No: 583-598
Website: https://aaasjournals.com/index.php/ajapas/index
ISI 2025: 1.126 SJIFactor 2024: 6.752 معامل التأثير العربي: 1.62

Design and optimization of active solar Heating system subjected to Tripoli microclimate

G. E. A. Muftah [1*], Nisreen Issa Aboujnah [2]
[1] Physics department, Faculty of science, University of Bani Waleed, Bani Waleed, Libya
[2] Energy management department, Faculty of engineering, University of Tripoli, Libya

تصميم منظومة طاقة شمسية نشطة وفقا للمناخ المحلي لطرابلس- ليبيا لهدف تسخين المياه المنزلية

جعفر الصيد عوض [1 *] ، نسرين عيسى أبوجناح [2]
[1] قسم الفيزياء، كلية العلوم، جامعة بني وليد، بني وليد، ليبيا
[2] قسم إدارة الطاقة، كلية الهندسة، جامعة طرابلس، ليبيا

[*]Corresponding author: muftah-geam4676@hotmail.com

Received: September 08, 2025	Accepted: November 19, 2025	Published: November 29, 2025

Abstract:
In order to design liquid Solar Water Heating (SWH) Systems under Tripoli microclimate conditions, the typical correlation based methods incorporate with the f- chart method were employed. It is normally used this methods because of its capability to evaluate the heat load fraction provided by the solar heating system. This methods are perfect in optimizing the solar collectors area for standard Configuration for SWH system. The Combine f-chart with the LCS was utilized, to define the optimum design and cost of the system. In this study, the effect of collector orientation on the overall performance of SWH system was considered, alteration of a fraction of the total load provided by insolation energy and an optimum collector size for the desired load was founded. Detail information about solar radiation availability is required for design and economic evaluation of a solar energy system. Long-term solar radiation measurements for Tripoli city are available and can be obtained. In this work, we analyzed the solar energy resource potential for Tripoli in order to design a suitable and optimal solar flat plate collector for residential use.
The purpose of this work is to design or size and optimize solar space and water heating system (active solar heating system) in order to convert solar energy into hot water and distribute it into the domestic proposes. For which, the microclimate of Tripoli will be analysed and the f-chart method is employed. Since the flat plate collector is expensive, the economic analysis is taken place. At the end , the size and parameters of solar heating system will be optimized for this particular location.

Keywords: Insolation energy, Solar Water Heating system, f- chart method, Economic analysis LCS, Tripoli, Libya.

الملخص
لتصميم أنظمة تسخين المياه بالطاقة الشمسية السائلة (SWH) في ظل الظروف المناخية المحلية لمدينة طرابلس، استُخدمت أساليب العلاقات الرياضية، بالإضافة إلى مخطط f . تُستخدم هذه الأساليب عادةً لقدرتها على تقييم نسبة الحمل الحراري التي يوفرها نظام التسخين الشمسي. تُعد هذه الأساليب مثالية لتحسين مساحة المجمعات الشمسية وفقًا للتكوين القياسي لنظام تسخين المياه بالطاقة الشمسية. استُخدم مخطط f المدمج مع مخطط LCS لهدف تحديد التصميم الأمثل وتكلفة النظام. في هذه الدراسة، تم دراسة تأثير اتجاه المجمع على الأداء العام لنظام تسخين المياه بالطاقة الشمسية، وتعديل نسبة الحمل الإجمالي التي توفرها طاقة الإشعاع الشمسي، وتم تحديد الحجم الأمثل للمجمع للحمل المطلوب. يتطلب تصميم نظام الطاقة الشمسية وتقييمه اقتصاديًا معلومات تفصيلية حول توافر الإشعاع الشمسي. تتوفر قياسات الإشعاع الشمسي طويلة المدى لمدينة طرابلس ويمكن الحصول عليها. في هذا السياق، قمنا بتحليل إمكانات موارد الطاقة الشمسية لطرابلس من أجل تصميم مجمع

شمسي مسطح مناسب ومثالي للاستخدام السكني. بشكل عام يهدف هذا العمل إلى تصميم أو تحديد حجم وتحسين نظام تسخين المياه بالطاقة الشمسية لتحويل الطاقة الشمسية إلى مياه ساخنة وتوزيعها على الاحتياجات المنزلية. وسيتم في هذا الصدد تحليل مناخ مدينة طرابلس المحلي، واستخدام طريقة الرسم البياني .f ونظرًا لارتفاع تكلفة المجمع الشمسي ذي اللوحة المسطحة، فقد أُجري تحليل اقتصادي.

الكلمات المفتاحية: الطاقة الشمسية، المجمعات الشمسية، أنظمة- f، تسخين المياه بالطاقة الشمسية، مخطط LCS.

Introduction

The proper design of SWH systems is an important to assure good performance and maximize the economic benefits of these systems as a large systems is required. Optimizing a SWH system includes different components such as collector area, solar insolation and hot water demand needs a proper method. There are many studies in the literature that address the design method of these systems. These design methods can be broadly classified into two categories, namely, correlation-based methods and simulation-based methods. The typical correlation based methods include the $f-$chart method, and $\emptyset-f$ chart methods have been widely used in preliminary design due to their convenience and inexpensiveness in predicting long-term performance compared to detailed simulation-based methods [1,2,3]. furthermore, a number of simulation-based methods like TRNSYS [5] and SOLCHIPS [5,6]. Have been utilized for the design of SWH systems. Application of utilizability method for solar hot water systems depends on determination of constant critical radiation intensity has been published by many Key researchers [6, 7, 8, 9, 10, 11].

Despite extensive studies and investigations that have been made in the world so far on SWH systems, Libya needs some more research. Utilizing solar water heaters in Libya started earlier at the beginning of the 1980's. Until recently one can say that there is no real large-scale implementation of such technology neither in the residential nor in the industrial sectors of Libya. Total systems installed over the past 35 years counted for less than 8000 systems,over third of them was in the Al Burayqah oil city [12]. The most significant installations are given below. Despite studies and investigations that have been made so far on SWH systems, Libya needs some more research in this field.

Implementation of these technologies would deliver advantages for the Libyan environment, economy, and society. Further, this would contribute to climate-political requirements at the global level [13].

Theoretical aspect

The angle between the earth‑sun line (through their centers) and the plane through the equator is called the solar declination, δ. The declination varies between −23.45 on December 21 to +23.45 on June 21. The solar declination may be estimated by Cooper's equation [14]:

$$\delta = 23.45\ \sin\left[360 \times \frac{284+n}{365}\right] \qquad (1)$$

Where n is the day of year (i.e. n =1 for January 1, n =32 for February 1, etc.).

Due to Earth's elliptic orbit around the Sun the actual solar radiationoutside the atmosphere at a given time (extraterrestrial radiation) will differ from G_{SC}. Over the year, it varies in the range of ±3.3% from the mean value[15]. This can be expressed mathematically as:

$$G_{0n} = G_{SC}\,(1 + 0.033\ \times\ \cos(360\frac{d}{365})) \qquad (2)$$

Where (d) is the day of the year. The subscript 0 denotes zero air mass (AM0) and the monthly average daily radiation on tilted surface, $\bar{H}_T$, can be expressed [15]:

$$\bar{H}_T = \bar{R}\,\bar{H} \qquad (3)$$

$\bar{H}$ is the monthly average daily radiation on horizontal surface.

$\bar{R}$ is the ratio of the monthly average daily radiation on a tilted surface to that on a horizontal surface for each month.

$\bar{R}$ can be expressed [15];

$$\bar{R} = \left(1 - \frac{\bar{H}_d}{\bar{H}}\right)\bar{R}_b + \frac{\frac{\bar{H}_d}{\bar{H}}(1+\cos\ s)}{2} + \frac{\rho(1-\cos\ s)}{2} \qquad (4)$$

The first term is the contribution of the beam radiation, the second tern is the contribution of diffuse radiation from the sky, and the third term is the contribution of radiation reflected in to the collector from the ground.

$\bar{H}_d$ is the monthly average daily diffuse radiation, $\bar{R}_b$ is the ratio of the monthly average beam radiation on the tilted surface to that on a horizontal surface for each month. (s) is a tilted surface from horizontal. ρ is the ground reflectance. Liu and Jordan suggest that ρ varies from 0.2 to 0.7 depending upon natural of the earth surface [16, 17].

Studies have shown that the fraction of the total radiation which is diffuse, $\frac{\bar{H}_d}{\bar{H}}$, is a function of $\bar{K}_T$ [15].

$$\bar{K}_T = \frac{\bar{H}}{\bar{H}_0} \qquad (5)$$

$$\frac{\bar{H}_d}{\bar{H}} = 1.39 - 4.03\bar{K}_T + 5.53\bar{K}_{T^2} - 3.11\bar{K}_{T^3} \qquad (6)$$

$\bar{R}_b$ is a monthly average ratio of extraterrestrial radiation on the tilted surface to that on a horizontal surface. It is estimated for flat collector facing directly towards the south. ∅ is a latitude ,and β a collector slope [2].

$$\bar{R}_b = \frac{\cos(\emptyset - s)\cos\delta\sin\omega_s' + (\frac{\pi}{180})\omega_s'\sin(\emptyset - s)\sin\delta}{\cos\emptyset\cos\delta\sin\omega_s + (\frac{\pi}{180})\omega_s\sin\emptyset\sin\delta} \qquad (7)$$

Where

ω_s is the sunset hour angle on a horizontal surface given by;

$$\omega_s = \text{ar}\cos\ (-\tan\emptyset\ \times\tan\delta) \qquad (8)$$

ω_s' is the sunset hour angle on the tilted surface given by;

$$\omega_s' = \text{MIN}\ [\omega_s, \text{ar}\cos\ (-\tan(\emptyset - s)\ \times\tan\delta)] \qquad (9)$$

The ratio of the monthly average transmittance-absorptance product $\overline{(\tau\alpha)}$ to the transmittance-absorptance product at normal incidence , $(\tau\alpha)_n$,could be estimated as a function of weighted average for the beam, diffuse , and reflected components of the radiation [15].

$$\frac{\overline{\tau\alpha}}{(\tau\alpha)_n} = \left(1 - \frac{\bar{H}_d}{\bar{H}}\right)\times\frac{\bar{R}_b}{\bar{R}}\times\frac{(\overline{\tau\alpha})_b}{(\tau\alpha)_n} + \frac{\bar{H}_d}{\bar{H}}\times\frac{1}{\bar{R}}\times\frac{1+\cos\beta}{2}\times\frac{(\overline{\tau\alpha})_d}{(\tau\alpha)_n} +$$

$$\rho_g\times\frac{1}{\bar{R}}\times\frac{1-\cos\beta}{2}\times\frac{(\overline{\tau\alpha})_g}{(\tau\alpha)_n} \qquad (10)$$

Where $(\overline{\tau\alpha})_b, (\overline{\tau\alpha})_d$, and $(\overline{\tau\alpha})_g$ are the monthly average values of the transmittance-absorptance product corresponding to beam, diffuse , and ground- reflected radiation.

$(\tau\alpha)$ is approximately 1% greater than the product of τ and α. Since surface radiation properties are seldom known to within 1%, the effective transmittance-absorptance product can be approximated for collectors with ordinary glass by;

$$(\tau\alpha) \cong 1.02\,\tau.\alpha \qquad (11)$$

For the diffuse and ground reflected components of radiation at the effective incidence angles at β, the mean incidence angles can be obtained from;

$$\theta_d = 59.68^\circ - 0.1388\beta + 0.001497\beta^2 \qquad (12)$$
$$\theta_g = 90^\circ - 0.5788\beta + 0.002693\beta^2 \qquad (13)$$

For tilted collector, the average angle of incidence for diffuse radiation should be less or equal 60°, while the average angle of incidence for the ground-reflected radiation should be more than 60°. As a conservative assumption, the average angle for diffuse radiation may be taken as 60°. The small contribution of ground-reflected radiation is also taken as having an average incidence angle of 60°. Then $\frac{(\overline{\tau\alpha})_d}{(\tau\alpha)_n}$, $\frac{(\overline{\tau\alpha})_g}{(\tau\alpha)_n}$ and $\frac{(\overline{\tau\alpha})_n}{(\tau\alpha)_n}$ could be calculated in same manner.

$$\frac{(\overline{\tau\alpha})_{d,g\text{ or }n}}{(\tau\alpha)_n} = 1 + b_0((1/\cos\theta) - 1) \qquad for \quad 0 \ll \theta \ll 60^\circ \qquad (14)$$

$$\frac{(\overline{\tau\alpha})_{d,g\text{ or }n}}{(\tau\alpha)_n} = 2(1+b_0)\cos\theta \qquad for \quad 60^\circ \ll \theta \ll 90^\circ \qquad (15)$$

Where
b_0 is incidence angle modifier coefficient from ASHRAE 93-77 test (b_0 ispositive for a flat-plate collector). θ is incidence angle, angle between beam radiation on a surface and the normal to that surface. For the beam component the effective angle of incidence $\bar{\theta}_b$, also called mean incidence
Angle for beam radiation, can be obtained from the original figures of Klein (1979) [3] as a function of collector slope, month, latitude, and azimuth angle (shown in figure 1). For Surfaces facing directly towards the equator it can be approximated as the incidence angle at 2.5 hours from solar noon on the average day of the month.

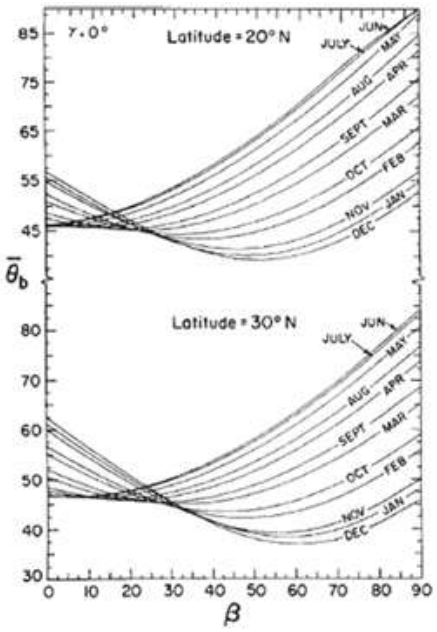

Figure 1 Monthly average beam incidence angle [3].

In order to estimate the space heating load of an apartment, the degree-day method is employed. This method is established upon the fact that the amount of heat needed to preserve a comfortable inside the apartment temperature is dependent upon the difference between the inside and outside temperatures. The average monthly space heating load, L_s, for an apartment fixed at 22 C is presumed to be proportional to the number of degree-days over the month [15].

$$L_s = DD \times UA \qquad (16)$$

Where

DD is the number of degree-days in a month. UA Is the building overall energy loss coefficient-area product. UA Must be calculated from the details of the building construction [15].

$$UA = \frac{\text{Design heatins load}}{\text{Design temperature difference}} \qquad (17)$$

The monthly water heating load, L_W can thus be estimated as

$$L_W = N \times (\#\ of\ persons) \times 100 \times (T_W - T_m) \times \rho \times C_P \qquad (18)$$

N is the number of days in the month. T_W is the minimum acceptable temperature for hot water; approximately 60C (140F). T_m is the mains supply water temperature. ρ is the density of water (1 kg/liter) C_P is the specific heat of water (4190 j/kg-c)
The monthly total load, L is the sum of the space and domestic water heating loads.

$$L = L_S + L_W \qquad (19)$$

Solar liquid collectors are most appropriate for central heating. They are the same as those used in solar domestic water heating systems. Flat-plate collectors are the most common, Figure 2 displays a standard configuration of SWH System covered by the f-chart method.

This system may use water or an anti freeze solution. a heat exchanger is used between the collectors and the tank to transfer heat from the collector in case an anti freeze fluid is used. The preheated tank utilized hot water for use any time later. If hot water is not as required load, the auxiliary tank could be used [16].

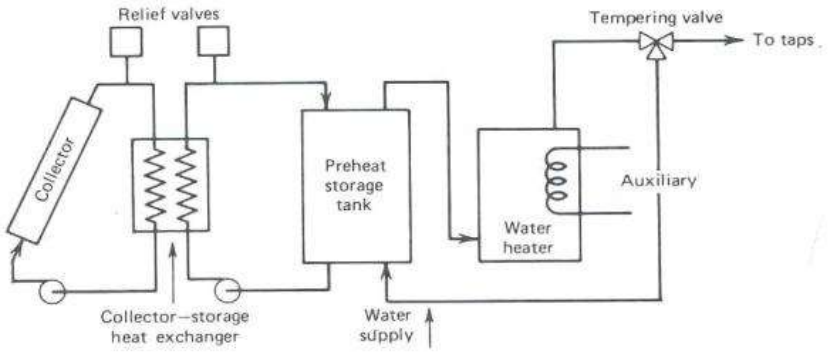

Figure 2 standard Configuration for SWH system [15].

The F-chart method estimates the fraction of a total heating load that will be provided by insolation energy for a standard Configuration for SWH system. Three variables should be taken in f-chart; firstly design function is collector area; secondary function is collector types, storage capacity, fluid flow rates, and collector heat exchanger sizes. The resulting correlations give the fraction of the monthly heating load (for space heating and hot water) supplied by solar energy (f), as a function of two dimensionless variables; X: ratio of collector losses to heating loads and Y: ratio of absorbed solar radiation to heating loads [16]. The key parameters in this method are represented by dimensionless groups, X and Y [15].

1- X:

- Definition: X is the ratio of collector energy loss during a month to the total heating load during a month.
- Mathematical expression:

$$X = \frac{(\text{Collector energy loss during a month})}{(\text{Total heating load during a month})} \qquad (20)$$

- Calculation:

$$X = F_R U_L \times \frac{F'_R}{F_R} \times (T_{ref} - \overline{T}_a) \times \Delta t \times \frac{A_C}{L} \qquad (21)$$

2- Y:

- Definition: Y is the ratio of the total energy absorbed on the collector plate during a month to the total energy load during a month.
- Mathematical expression :

$$Y = \frac{(\text{Total energy absorbed on the collector plate during a month})}{(\text{Total energy load during a month})} \qquad (22)$$

- Calculation:

$$Y = F_R(\tau\alpha)_n \times \frac{F'_R}{F_R} \times [\frac{\overline{(\tau\alpha)}}{(\tau\alpha)_n}] \times \overline{H}_T \times N \times \frac{A_C}{L} \qquad (23)$$

3- f:

- Definition: f is the fraction of monthly heating loads (for space heating and hot water) supplied by solar energy.
- Mathematical expression :

$$f = 1.029Y - 0.065X - 0.245Y^2 + 0.0018X^2 + 0.0215Y^3 \qquad (24)$$

4- Other parameters :

- A_C is area of solar collector (m^2)
- F'_R is collector-heat exchange efficiency factor (%)
- F_R is collector heat removal factor (%)
- U_L is collector overall energy loss coefficient ($W/m^2 - ℃$)
  Δt is total number of seconds or hours in the month
- $\overline{T}_a$ is monthly average ambient temperature (℃)

- L is monthly total heating load (GJ)

- $\bar{H}_T$ is monthly averaged daily radiation incident on collector surface per unit area (MJ/m^2)
- N is number of days in the month
- $\tau\alpha$ is monthly average Transmittance-absorptance product (%)
- $(\tau\alpha)_n$is normal transmittance-absorptance product (%)
- T_{ref} is reference temperature (100℃)

Result and discussion

In order to size and optimize the flat plate collector system for supply a house contained five people by hot water, the out lined the basic characteristic of insolation and other microclimate data of Tripoli have been collected. The insolation (direct, diffuse and reflection insolation), the ambient temperature, albedo and sun duration on horizontal surface are presented in table 1. The data has been requested from research centre of solar energy in Tripoli. These data were collected using pyranometer instrument. It was mounted for one year meteorological. The data was automatic recorded every 10 minutes. In additional it is an important to obtain measurable data from the field where the solar heating system should be applied, in order to achieve reasonable study.

Table 1. Main monthly weather data of Tripoli city.

Month	Ta	Gr	Gt	DNI	Gd	RFR	Alpedo	SD
	°C	MJ/m^2day						hr
Jan	11.33	10.590516	15.841944	7.659936	4.15602	2.018232	0.37	5.7
Feb	11.91	13.2624	17.468532	13.601664	5.728896	2.500308	0.43	5.1
Mar	14.93	18.388008	21.278916	18.9432	6.510852	3.305628	0.33	7.2
Apr	18.55	23.160492	22.656672	20.338308	8.486892	4.0428	0.36	9.8
May	21.03	25.504128	22.06404	25.013808	7.774956	4.90266	0.41	10.7
Jun	27.98	27.531684	22.349268	25.418664	8.59662	4.30056	0.39	11
Jul	29.02	29.069604	24.03018	31.89348	6.764868	4.423572	0.42	12.7
Aug	29.1	26.32842	24.544152	28.615968	6.814332	3.873204	0.35	10.6
Sep	27.28	21.417444	23.574672	23.079492	6.966864	3.22182	0.32	8.9
Oct	23.62	15.506892	19.753272	17.716428	6.098256	2.156148	0.3	6.8
Nov	18.07	12.598992	18.948816	15.89724	4.802508	1.656972	0.25	6.1
Dec	15.47	9.9054	15.889176	12.66066	7.723368	1.409724	0.28	5.6
Yearly	**20.69**	**19.438668**	**20.7**	**20.07**	**6.702048**	**3.150972**	**0.35**	**8.4**

Figure 2 shows monthly average daily temperature. As can be seen that the shape forms a semi-curve, the peak temperatures takes place during summer time (from June to September) indicating the average of sunshine duration is high. In contrast monthly average daily temperature in winter time is low indicating average daily of sunshine duration is low (December, February, and January). Between two the sedurations, temperatures are varied. Within the spring and autumn duration, the temperature is in middle. This information is an important for a designer who wants to size and optimize the flat plate collector system for supply a house by hot water.

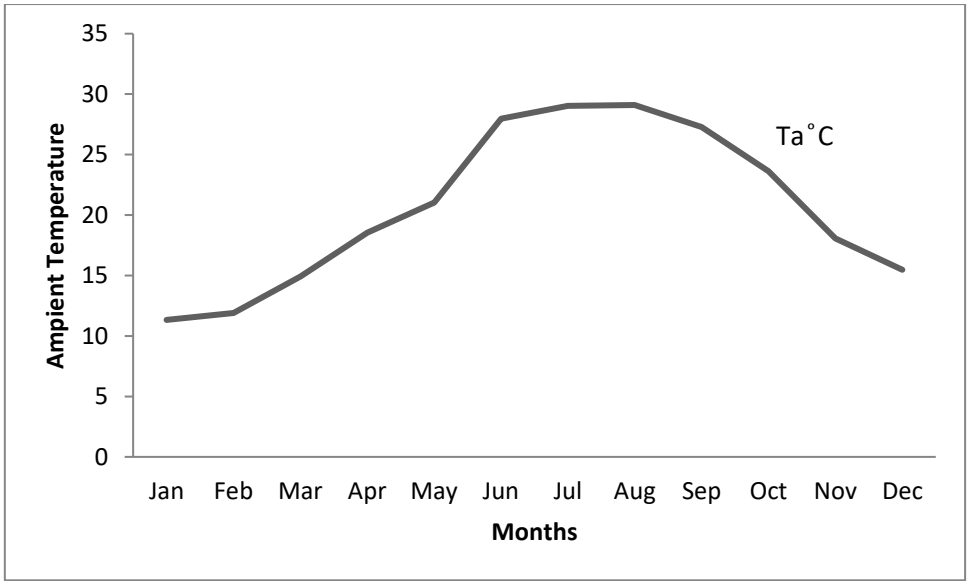

Figure 2. Average daily ambient temperature for the year 2019/2020 in Tripoli

Monthly average daily insolation at horizontal surface in side our atmosphere is displayed in figure 3. It is obvious that the insolation distribution varies between 9 MJ/m^2day and 29 MJ/m^2day. This divergence is a quite large, as the measurements have been taken on horizontal surface. In this case large size of the collector is required at winter whereas small size is desirable at summer time. As a result there will be a large difference in collector size. Therefore the deviation between the insolation has to be reduced as possible as could.

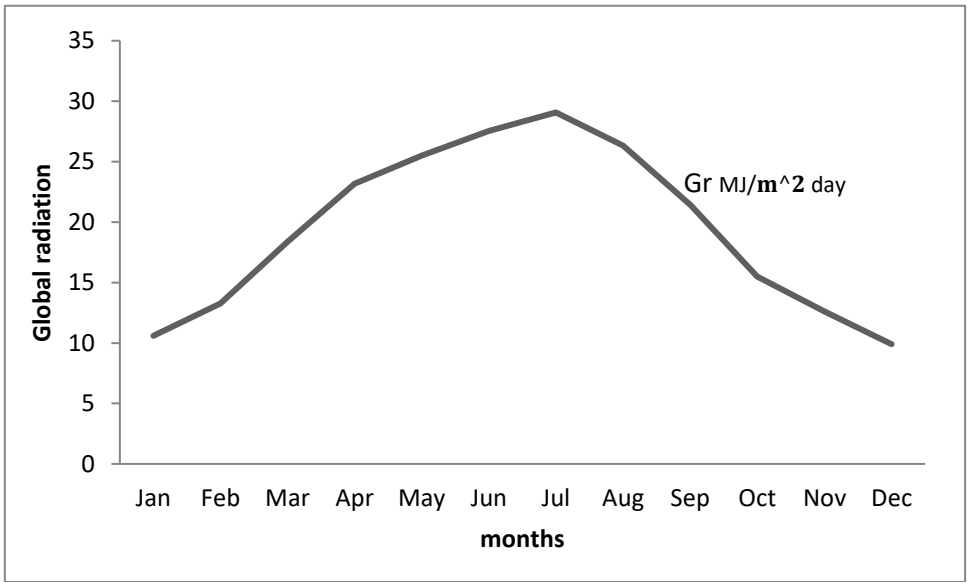

Figiure 3. Daily solar insolation for the year 2019/2020 in Tripoli

The monthly average daily extraterrestrial $(\bar{H}_0)$and monthly average daily terrestrial $(\overline{H_t})$ insolation on horizontal surface in Tripoli city presented in figure 4. It is clear that the insolation at outside our atmosphere is larger than insolation inside atmosphere indicating the inside atmosphere has been effecting on the insolation. That is because, while it is passing the atmosphere, the insolation is spitted into many parts; reflected towards the space, Scattered in all directions (absorbed and re-emitted as IR in all the directions from the molecules in the atmosphere), and direct radiation reaching the earth's surface.

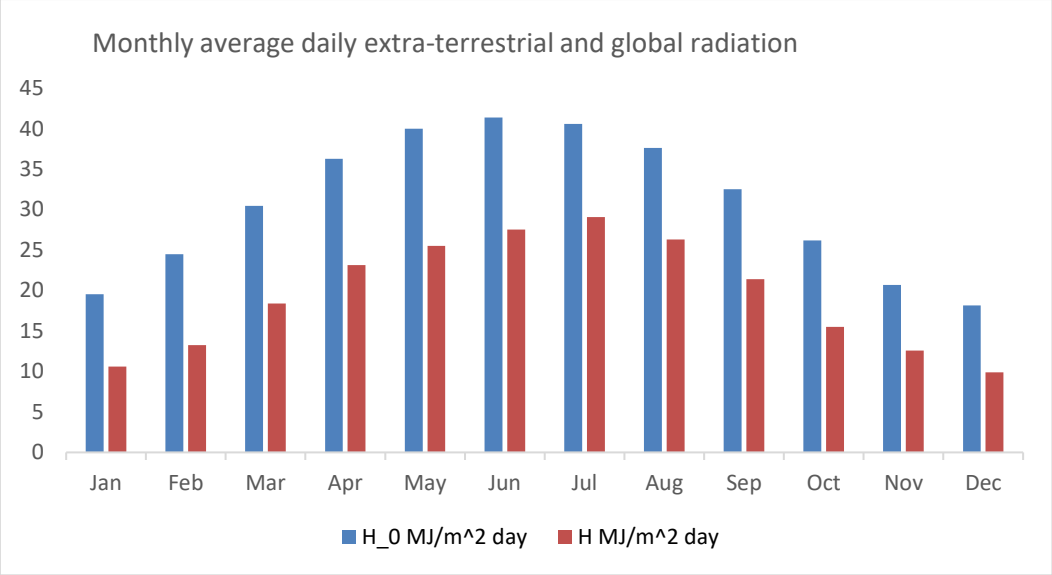

Figure 4. Monthly average daily global radiation (H) and monthly averaged extra-terrestrial daily radiation (Ho) on a horizontal surface in Tripoli.

In order to accumulate all parts of insolation that reaches into horizontal surface inside our atmosphere, the monthly average daily beam ($\bar{H}_b$), diffuse ($\bar{H}_d$), reflection($\bar{H}_r$) and global ($\bar{H}_t$) insolaslation have been analyzed and plotted in figure 5. The global insolation is sum of effect solar radiation (beam, diffuse, reflection radiation). It is obvious that the beam insolation part contributes by a largest amount in global insolation. By the way the beam insolation is the most need in order to produce more energy from the surface. However, there is no much contribution from the reflected inslation portion because the surface position is horizontal so far.

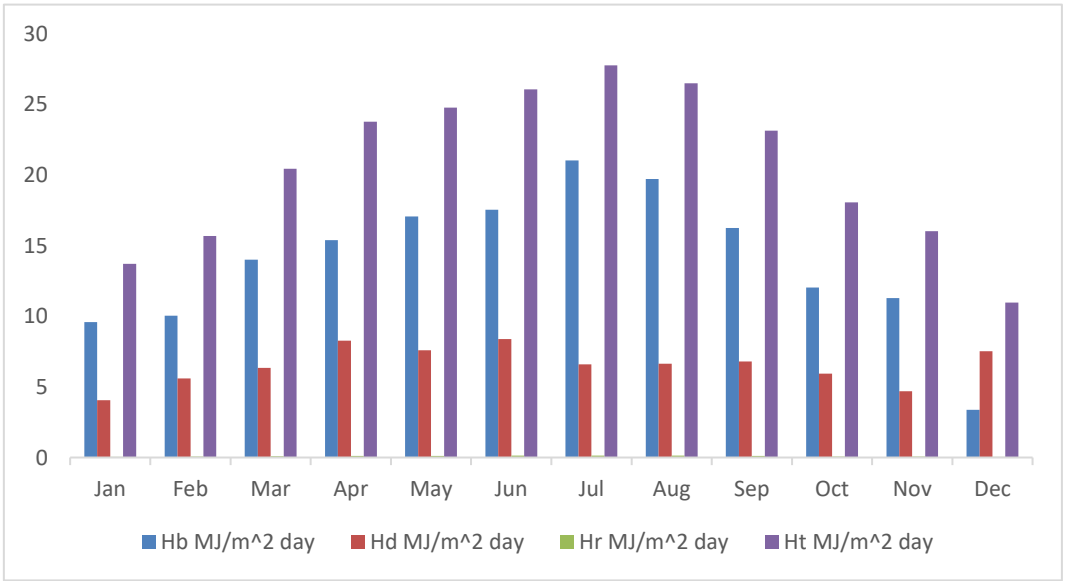

Figure 5, Monthly average daily global radiation (H), beam radiation (Hb) and diffuse radiation (Hd) on a horizontal surface in Tripoli city.

In order to maximise the direct-beam insolation onto a flat plate solar collector, it is required to incline the plate around two dimensions, namely the tilt and the plate azimuth angle, which should require two motors. But, in general, the marginal energy gains from tracing the azimuth angle are low. Hence, the second best option is to keep the slope flexible, but facing due south.

In most of the cases, it is not possible to move the surface at all; the theoretical optimal tilt angle giving the maximum amount of direct beam radiation is around to the site's latitude. Tilting the surface up, however, causes the diffuse light portion to decrease. The optimal tilt angle for sites with humid climates is therefore 10 – 25% less than the latitude. In Germany, for instance, at 48°N, a tilt angle of 30° would be optimal, whereas in Spain, it could be up to 40°[18].

In this case the azimuth surface angle (a south facing surface) is assumed to be zero and plate tilted angle has to be optimized. The affection of applied different tilted angles on the estimation of monthly average of daily insolation into a south facing plate is obtained and analyzed.

Table 2 illustrates the worksheet insolation on tilted plate (φ -β = -15°). As can be seen from the worksheet, monthly average daily terrrestial insolation values, $\overline{H}$ (column G2) and corresponding values of clearness index, $\overline{K}_T$ (column G3) for Tripoli can be calculated by dividing $\overline{H}$ by the montly average daily extraterrestrial insolation $\overline{H}_o$ which is presented in correlation 6.

The ratio of diffuse to globle insolation,$\overline{H}_d/\overline{H}$ (column G4) is found for each month using correlation 6. Values of $1-\overline{H}_d/\overline{H}$ are presented in column G5. The product of $1-\overline{H}_d/\overline{H}$ in column G5 and tlited beam factor,$\overline{R}_b$(column G6), gives the contribution of beam component. $\overline{R}_b$ is found by using correlation 7. The product of $\overline{H}_d/\overline{H}$ (column G4) and $(1+cos\ \beta)/2$ (item D) gives the diffuse contribution (column G8). Total tilited factor $\overline{R}$ is the sum of the contributions of beam (column G7), diffuse (column G8) components and the reflected component (item F). The monthly average daily insolation on the tilted surface $\overline{H}_T$ (column G10) is the product of $\overline{H}$ (column G2) and $\overline{R}$ (column G9).

Table (2) Worksheet for calculating the monthly average daily insolation on the tilted plate $\overline{H}_T$ at φ -β = -15°

B. Latitude : φ = 32.88° **C**. Inclination : β = 47.88° **A**. Location: Tripoli

D. (1+Cos β)/2 = 0.835 **E**. Ground Reflection ρ = 0.2 **F**. ρ (1 –cosβ)/2 = 0.0329

G1.	G2.	G3.	G4.	G5.	G6.	G7.	G8.	G9.	G10.
Month	$\overline{\mathbf{H}}$ **MJ /m²day**	$\overline{\mathbf{K}}_\mathbf{T}$	$\overline{\mathbf{H}}_\mathbf{d}/\overline{\mathbf{H}}$	$\mathbf{1-\overline{H}_d/\overline{H}}$	$\overline{\mathbf{R}}_\mathbf{b}$	**Beam (G5.×G6.)**	**Diffuse (D.×G4.)**	$\overline{\mathbf{R}}$ **(G7.+G8.+F.)**	$\overline{\mathbf{H}}_\mathbf{T}$ **MJ /m²day (G9.×G2.)**
Jan	10.59	0.27	0.64	0.360693673	1.976	0.713	0.534	1.280	13.553
Feb	13.26	0.34	0.53	0.466702801	1.592	0.743	0.445	1.222	16.200
Mar	18.39	0.48	0.39	0.614901353	1.222	0.751	0.322	1.106	20.334
Apr	23.16	0.62	0.28	0.72334786	0.912	0.660	0.231	0.924	21.399
May	25.50	0.70	0.22	0.783762631	0.723	0.567	0.181	0.780	19.900
Jun	27.53	0.76	0.16	0.840237206	0.647	0.544	0.133	0.710	19.546
Jul	29.07	0.80	0.12	0.88346856	0.680	0.601	0.097	0.731	21.250
Aug	26.33	0.72	0.20	0.802867478	0.826	0.663	0.165	0.861	22.668
Sep	21.42	0.58	0.30	0.696735737	1.088	0.758	0.253	1.045	22.372
Oct	15.51	0.43	0.44	0.563646561	1.462	0.824	0.365	1.221	18.937
Nov	12.60	0.34	0.53	0.469763613	1.867	0.877	0.443	1.353	17.046
Dec	9.91	0.27	0.65	0.354662854	2.104	0.746	0.539	1.318	13.056

In order to obtainthe monthly average daily diffuse insolation fraction $\overline{H}_d/\overline{H}$, the correlation 6 is employed. As can be seen from the equation, the $\overline{H}_d/\overline{H}$I s a fuction of a clearness index $\overline{K}_T$. It is noticeable from the figure 6 that as $\overline{K}_T$ decrease, the $\overline{H}_d/\overline{H}$ increase.Table 2, G3-columm shows that the largest $\overline{K}_T$ values are during summer time; for July the $\overline{K}_T$ is found to be 0.80 indicating the sky is clear and more energy is available on earth surface with 23 MJ/m^2-day as shown in figure 7. Lowest values are found at January and December with 0.27. This indicats that the atmospere is unclear with low insolalion value with about 14 MJ/m^2-day .Therefore the diffuse radiation will be large but the energy incidcedent is lowas tublated in G8 columm.

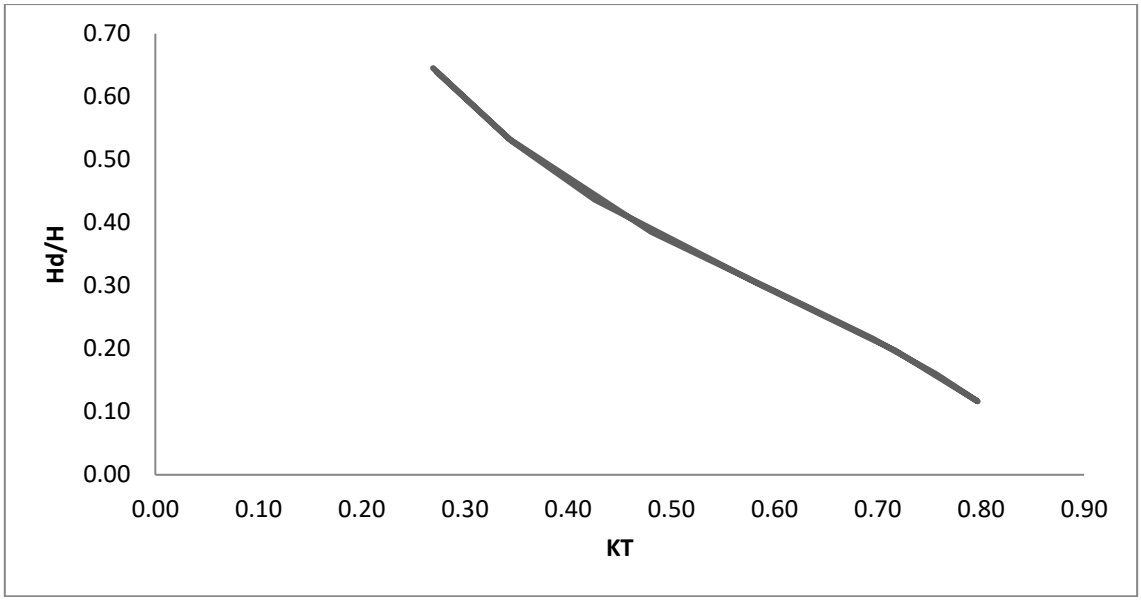

Figure 6. Monthly average daily diffuse insolation fraction verse Clearness index.

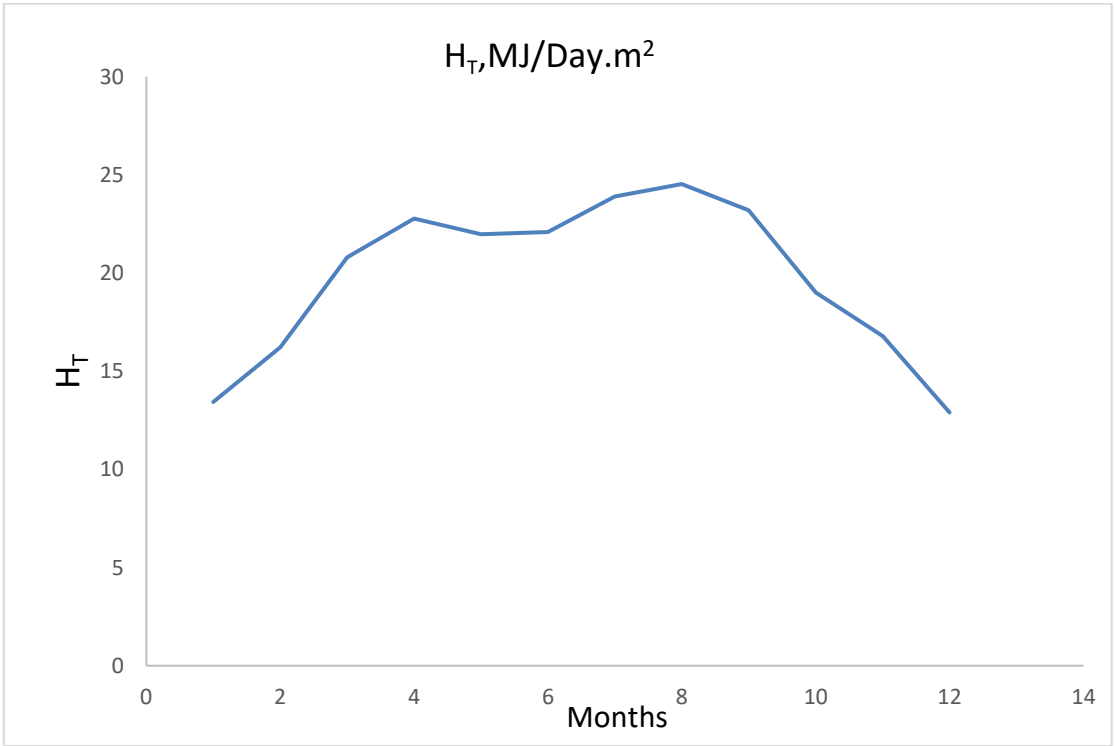

Figure 7. Monthly avearge daily inslation on tilted plate at β = 47.88° versus months of the year.

Table 3, Worksheet for calculating the monthly average daily insolation on the tilted plate $\overline{H}_T$ at φ -β = 0°.
A. Location: Tripoli . **B**. Latitude : φ = 32.88° **C**. Inclination : β = 32.88°
D. (1+Cos β)/2 = 0.9199 **E**. Ground Reflection ρ = 0.2 **F**. ρ (1 -cos β)/2 = 0.016

G1.	G2.	G3.	G4.	G5.	G6.	G7.	G8.	G9.	G10.
Month	$\overline{H}$ MJ /m²day	$\overline{K}_T$	$\overline{H}_d/\overline{H}$	$1-\overline{H}_d/\overline{H}$	$\overline{R}_b$	Beam (G5.×G6.)	Diffuse (D.×G4.)	$\overline{R}$ (G7.+G8.+F.)	$\overline{H}_T$ MJ /m²day (G9.×G2.)
Jan	10.59	0.27	0.64	0.360704934	1.795	0.648	0.588	1.252	13.255
Feb	13.26	0.34	0.53	0.466745295	1.514	0.707	0.491	1.213	16.092
Mar	18.39	0.48	0.39	0.614905255	1.243	0.764	0.354	1.135	20.864
Apr	23.16	0.62	0.28	0.723457477	1.014	0.734	0.254	1.004	23.257
May	25.50	0.70	0.22	0.784251796	0.869	0.682	0.198	0.896	22.860
Jun	27.53	0.76	0.16	0.84053879	0.810	0.681	0.147	0.843	23.215
Jul	29.07	0.80	0.12	0.882521505	0.836	0.738	0.108	0.862	25.047
Aug	26.33	0.72	0.20	0.802378837	0.949	0.761	0.182	0.959	25.255
Sep	21.42	0.58	0.30	0.696726145	1.145	0.798	0.279	1.093	23.410
Oct	15.51	0.43	0.44	0.563580126	1.419	0.800	0.401	1.217	18.872
Nov	12.60	0.35	0.53	0.470370381	1.715	0.807	0.487	1.310	16.506
Dec	9.91	0.27	0.64	0.356267001	1.889	0.673	0.592	1.281	12.689

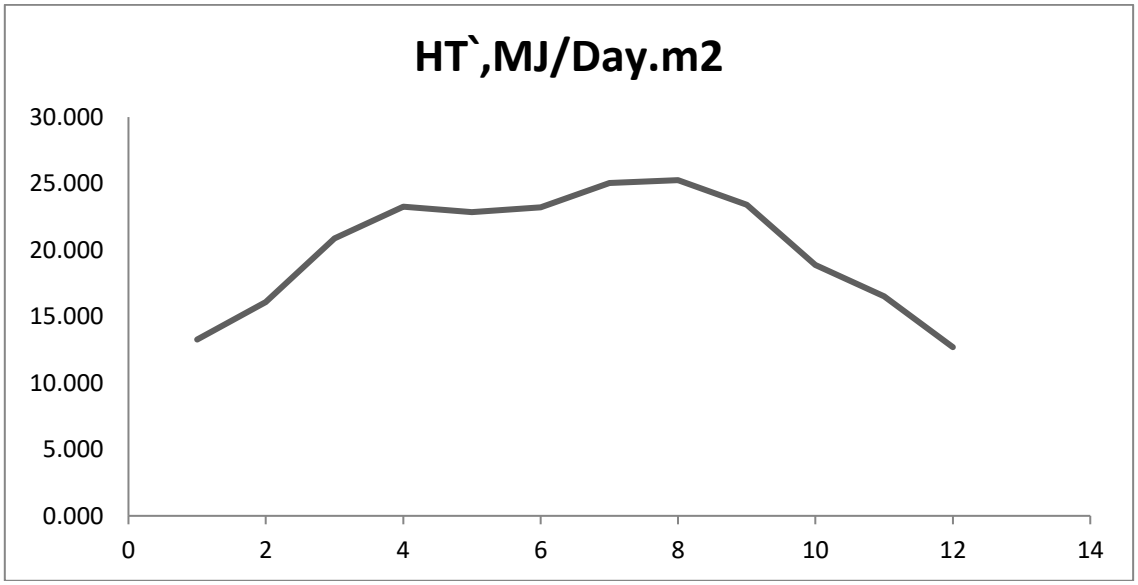

Figure 8 Monthly avearge daily inslation on tilted plate at β =32.88° (H_T) versus months of the year.

The monthly averages daily insolationn on a south facing plate tilted from horizontal in Tripoli at different tilted flate plate collectted is tublalated in table 4 $\overline{H}_T$. In order to have more visulize, $\overline{H}_T$ at different tilited angle vs. months for whole year is plotted and showed in figure 9. The surface was fixed toward south (Azemithal angle = 0). Incline the plate is need, such that the best insolation is optained. It is noticible from the figure that $\overline{H}_{T2}\overline{H}_{T5}\overline{H}_{T8}$ show highest available insolation energy during mid year whereas during January and December show lower available insolation energy in contrast with$\overline{H}_{T1}$, which shows low insolation energy at the mid if the year and a bit higher energy at Juanuary and december. The $\overline{H}_{T5}$has been chosen as the standard divation between lowest and largest insolation energy value indicating more reliability for a SWH designer.

Table 4 The monthly averages of daily radiation incident on a south facing plate inclined from horizontal in Tripoli at different inclination angles.

A. Location: Tripoli . B. Latitude : φ = 32.88°

Month	No. of Days	$\overline{H}$	s = 90° Vertical	S=47.88° φ -s =-15°	S=47.88° φ -s =-10°	S=47.88° φ -s =-5°	S=47.88° φ -s =0°	S=47.88° φ -s =5°	S=47.88° φ -s =10°	S=47.88° φ -s =15°
			$\overline{H}_{T1}$	$\overline{H}_{T2}$	$\overline{H}_{T3}$	$\overline{H}_{T4}$	$\overline{H}_{T5}$	$\overline{H}_{T6}$	$\overline{H}_{T7}$	$\overline{H}_{T8}$
		MJ/m^2 day								
Jan	31	10.59	11.166	13.553	13.523	13.423	13.255	13.021	12.721	12.358
Feb	28	13.26	12.552	16.200	16.251	16.215	16.092	15.884	15.592	15.218
Mar	31	18.39	13.779	20.334	20.628	20.805	20.864	20.806	20.630	20.339
Apr	30	23.16	11.334	21.399	22.143	22.764	23.257	23.619	23.847	23.939
May	31	25.50	8.284	19.900	20.991	21.981	22.860	23.619	24.256	24.764
Jun	30	27.53	6.895	19.546	20.864	22.092	23.215	24.225	25.114	25.877
Jul	31	29.07	7.448	21.250	22.638	23.904	25.047	26.064	26.939	27.671
Aug	31	26.33	10.544	22.668	23.664	24.528	25.255	25.838	26.273	26.557
Sep	30	21.42	13.812	22.372	22.852	23.198	23.410	23.484	23.421	23.221
Oct	31	15.51	14.253	18.937	19.022	19.000	18.872	18.637	18.298	17.857
Nov	30	12.60	14.147	17.046	16.971	16.788	16.506	16.144	15.690	15.150
Dec	31	9.91	10.973	13.056	13.030	12.899	12.689	12.440	12.115	11.730

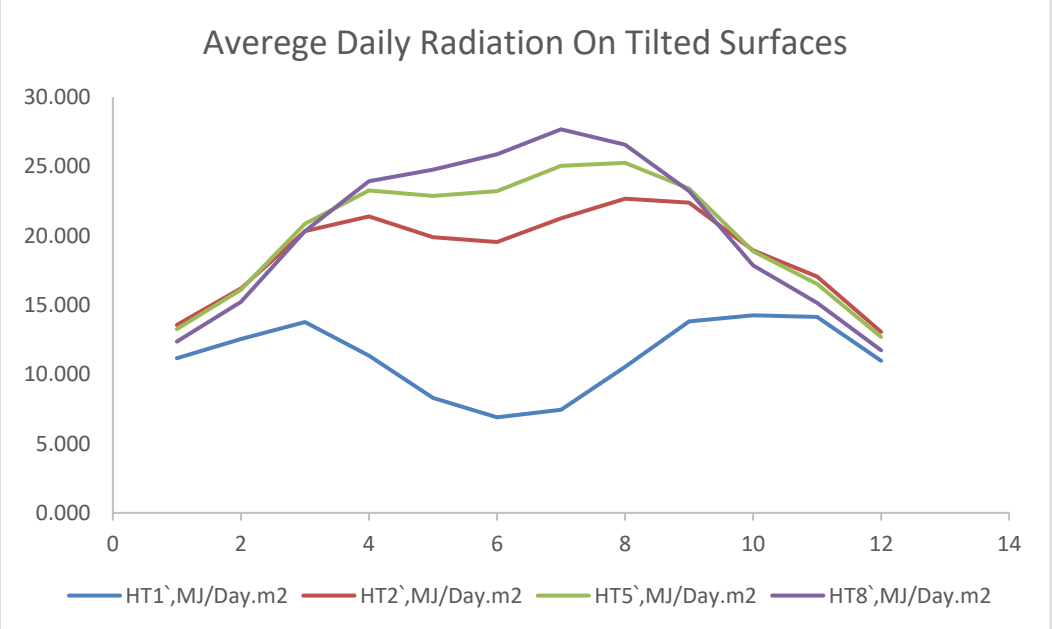

Figure 9, $\overline{H}_T$ at different tilited angle as a function of months for whole year.

As $(\overline{\tau\alpha})/(\tau\alpha)_n$ depends on the angle at which insolation hit collector plate, $(\overline{\tau\alpha})/(\tau\alpha)_n$has been analysised. The main point of present table 5 is to display $(\overline{\tau\alpha})/(\tau\alpha)_n$ for collector inclined at β = 32.88°. Flate plate solar collectors having two glass covers a flat back absober surface are considered toinstall a solar heating system located in Tripoli Libya (Latitude 32.88).

The monthly average incidence angle for beam radiation, $\bar{\theta}_b$ is found from correlation in figure 1 and tabulated in column 2. From which $(\overline{\tau\alpha})_b/(\tau\alpha)_n$ has been caculated using eqaution 14 and preesented in column 5. For diffuse radtion, the monthly average incidence angle $\bar{\theta}_d$ has been found using corrolation 12 and tabulated in column 3. From which the $(\overline{\tau\alpha})_d/(\tau\alpha)_n$ has been calculated and presented in column 6. For reflected radiation the monthly average incidence angle $\bar{\theta}_g$ has been established using corrolation 13, then $(\overline{\tau\alpha})_g/(\tau\alpha)_n$ has been calculated and presented in column 7.

Table 5, $(\overline{\tau\alpha})/(\overline{\tau\alpha})_n$ for collector inclined at β = 32.88°

Month	$\bar{\theta}_b$	$\bar{\theta}_d$	$\bar{\theta}_g$	$(\overline{\tau\alpha})_b/(\tau\alpha)_n$	$(\overline{\tau\alpha})_d/(\tau\alpha)_n$	$(\overline{\tau\alpha})_g/(\tau\alpha)_n$	$\bar{R}_b/\bar{R}$	Beam	Diffuse	Gr.Refl	$\overline{\tau\alpha}/(\tau\alpha)_n$
Jan	43	56.735	73.88	0.938	0.86	0.461	1.434	0.485	0.404	0.043	0.932
Feb	43	56.735	73.88	0.938	0.86	0.461	1.248	0.546	0.348	0.044	0.938
Mar	45	56.735	73.88	0.938	0.86	0.461	1.096	0.626	0.269	0.047	0.942
Apr	46	56.735	73.88	0.938	0.86	0.461	1.01	0.676	0.218	0.053	0.947
May	48	56.735	73.88	0.938	0.86	0.461	0.97	0.697	0.190	0.060	0.947
Jun	50	56.735	73.88	0.938	0.86	0.461	0.96	0.731	0.150	0.063	0.944
Jul	50	56.735	73.88	0.938	0.86	0.461	0.97	0.775	0.108	0.062	0.945
Aug	47	56.735	73.88	0.938	0.86	0.461	0.99	0.731	0.163	0.056	0.950
Sep	45	56.735	73.88	0.938	0.86	0.461	1.048	0.679	0.220	0.049	0.947
Oct	43	56.735	73.88	0.938	0.86	0.461	1.166	0.616	0.284	0.044	0.944
Nov	43	56.735	73.88	0.938	0.86	0.461	1.309	0.577	0.320	0.041	0.938
Dec	43	56.735	73.88	0.938	0.86	0.461	1.474	0.492	0.398	0.042	0.932

Table 6 presents the calculations the monthy space and haeting load using average daily degreeday mothod for each month. The estimation for the long-term monthly average space and heating loads are needed, as the amount of collector area depends strongly on the load, this calculations is an impotantant for the design procedures. For which the degree-day method has been empolyed.

Table 6 the monthy space and haeting load.

Tb=18.3°C (UA)h=375 W/c

Month	No. of Days	Ta` (c°)	σm	h	DD (c°-days)	Ls (GJ/month)	Lw (GJ/month) in 20.7 c	Lt (GJ/month)
Jan	31	11.33	1.56	0.8020	221.11	7.16	2.04	9.21
Feb	28	11.91	1.54	0.7821	183.49	5.95	1.84	7.79
Mar	31	14.93	1.46	0.4156	120.62	3.91	2.04	5.95
Apr	28	18.55	1.35	-0.0338	41.68	1.35	1.98	3.33
May	31	21.03	1.28	-0.3832	15.66	0.5072	2.04	2.55
Jun	30	27.98	1.08	-1.6393	0.1977	0.0064	1.98	1.98
Jul	31	29.02	1.05	-1.8373	0.1025	0.0033	2.04	2.05
Aug	30	29.1	1.05	-1.8551	0.0962	0.0031	2.04	2.05
Sep	31	27.28	1.1	-1.4927	0.3319	0.0108	1.98	1.99
Oct	31	23.62	1.2	-0.7933	4.004	0.1297	2.04	2.17
Nov	30	18.07	1.37	0.0308	49.33	1.60	1.98	3.57
Dec	31	15.47	1.44	0.3528	107.04	3.47	2.04	5.51
	365	20.69			743.67	24.10	24.05	48.14

Figure 10 shows the annual load fraction verus collector area which is known as f-chart . As can be seen the relation between them porpotions linerly for low collector areas. This indicates the energy supplied by the collector is consumed fully by system and the duming does not occur. But no doubt the the system needs more energy to deliver and extra collector area has to be install.

As the load fraction and collector area increase, the relation between them loses its linearity form indicting decrease atthe rate. In other words, the collector will deliver energy will not use it the load, i.e additional collecor area does not lead to equal additional load fraction met by system.

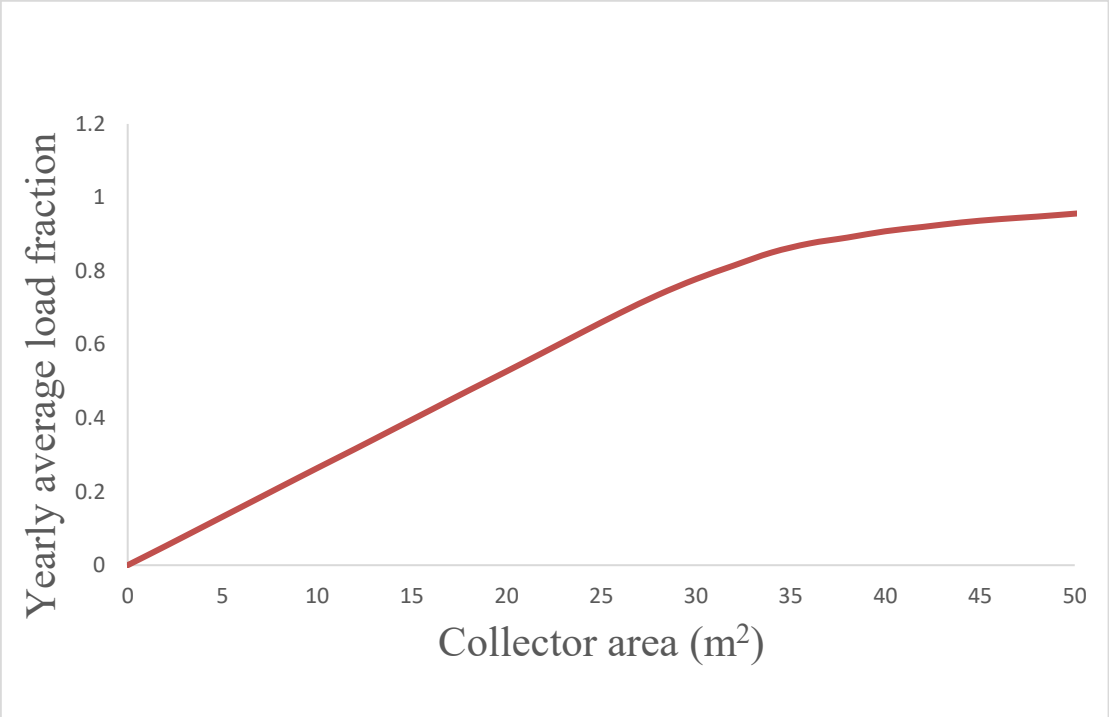

Figure 10 the annual load fraction verus collector area (f-chart curve). The correction factors values of the storage and load heat exchanger size have been chosen to be one.

Table 7 F-chart worksheet for solar heating load fraction.

month	Corrected X/A	Corrected Y/A	Area=25m2			Area=30m2			Area=35m2		
			X	Y	f	X	Y	f	X	Y	f
Jan	0.078	0.022	1.94	0.54	0.39	2.33	0.65	0.43	2.72	0.76	0.48
Feb	0.082	0.028	2.06	0.71	0.49	2.47	0.85	0.56	2.88	0.99	0.63
Mar	0.115	0.053	2.89	1.33	0.81	3.46	1.6	0.90	4.03	1.86	0.97
Apr	0.191	0.103	4.77	2.58	1.12	5.73	3.1	1.16	6.68	3.61	1.18
May	0.25	0.137	6.24	3.42	1.18	7.49	4.1	1.2	8.74	4.79	1.24
Jun	0.283	0.172	7.08	4.31	1.24	8.5	5.17	1.32	9.92	6.033	1.54
Jul	0.28	0.187	6.99	4.66	1.28	8.39	5.6	1.43	9.79	6.53	1.79
Aug	0.28	0.189	6.99	4.72	1.29	8.38	5.67	1.46	9.78	6.62	1.85
Sep	0.285	0.174	7.18	4.35	1.24	8.56	5.22	1.33	10	6.1	1.57
Oct	0.283	0.132	7.09	3.30	1.13	8.5	3.96	1.15	9.92	4.625	1.18
Nov	0.179	0.068	4.47	1.69	0.89	5.37	2.03	0.97	6.26	2.36	1.011
Dec	0.124	0.035	3.09	0.86	0.54	3.71	1.04	0.61	4.33	1.21	0.68
					f			f			f
					0.68			0.80			0.85

Figure 11 shows Life cycle savings (LSS). LCS inducates the net savings to the owener during the time of the solar energy system which is to be estimated based on past experience. Determine of optimum area, solar load fraction is based on life cycle savings. So we need to find out the max LCS and couble it with solar load fraction curve, in order to obtain the optimum area. The opimum value of collector area is 30 m2 givning solar fration of about 0.80. this means 80% of the load will be power by solar energy system and 20% by other enegy source.

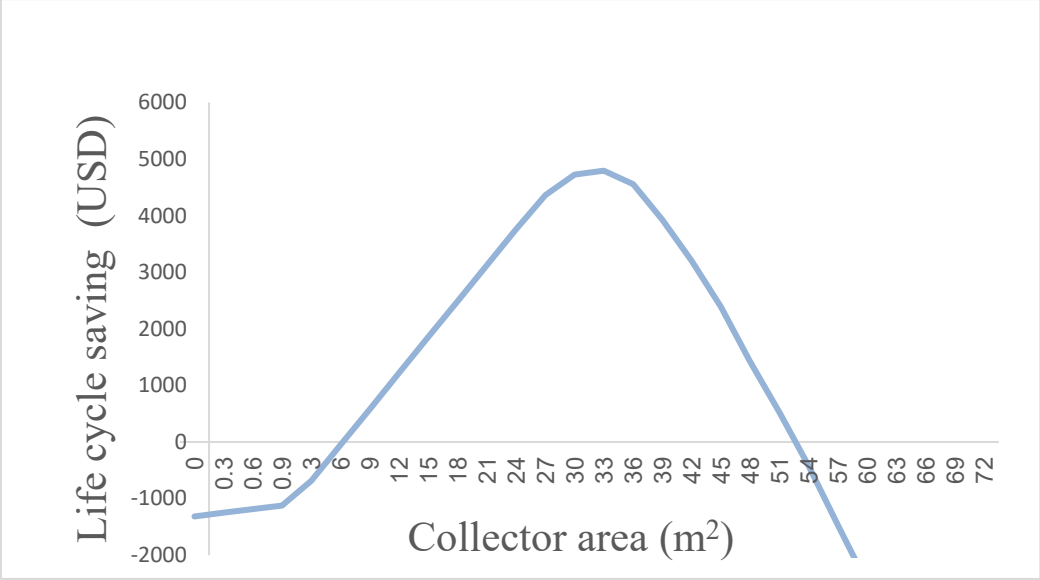

Figure 11 Life cycle savings (LSS).

Conclusion

In order to design solar heat system for space and water heating load, the some paramters have been studied. The insolation on horizon and tilted plane has been discussed from which the optimum insolation angle was obtained 33.88° . Then the effective transmitance-absorptance product has been analyised and obtained. The space and heating load was calculated and they were veried with about 2 MJ/month to 9 MJ/month. The long term performance of solar heat was done for which solar fraction curve has been obtained analysised. At the end in order to have optimum design with best cost, economice analysises have included and mach with solar load fraction. The optimum area was 33 m^2. The 80% of the load was powerd by solar heating saystm.

Compliance with ethical standards

Disclosure of conflict of interest

The authors declare that they have no conflict of interest.

References

[1] Duffie, J.A. and Beckman, W.A. (1991) Solar Engineering of Thermal Processes. Wiley, Hoboken.
[2] Klein, S. A., A Design procedure for solar heating system, Ph. D university of Wisconsin-Madison, (1976).
[3] Klein, S. A., & Beckman, W. A. A general design method for closed-loop solar energy systems. Solar Energy, 22, (1979) 269-282.
[4] Klein, S. A., Beckman, W. A., & Duffie, J. A. (1975).
[5] Lund, P. D. A general design methodology for seasonal storage solar systems. Solar Energy, 42(3), (1989) 235-251.
[6] Lund, H., & Peltola, E.,SOLCHIPS: Simulation of Solar Heating Systems with Seasonal Storage, Proceedings of the International Conference on Solar Energy for Nordic Countries, Espoo, Finland, 1992.
[7] Gordon, J. M., & Rabl, A. (1982), Design, Analysis, and Optimization of Solar Collector Systems, Solar Energy, 29(6), 491–502.
[8] Barley, C. D. & Winn, C. B., "Optimal sizing of solar collectors by the method of relative areas", Solar Energy, Vol. 21, No. 4, pp. 279-289, 1978
[9] Buckles, W. E. & Klein, S. A., "Analysis of solar domestic hot water heaters", Solar Energy, Vol. 25, No. 5, pp. 417-424, 1980
[10] M. M. Hawas & M. R. Abou-Zeid (1983), "A general chart for sizing the collectors of solar heating systems", Energy Conversion and Management, Vol. 23(3): 135-140.

[11] Sergio Colle, Humberto Vidal, Upper bounds for thermally driven cooling cycles optimization derived from the f–chart method, Volume 76, Issues 1–3, January–March 2004, Pages 125-133, Solar Energy.
[12] Fatiha Abdul Rahman(2019), F-Chart Method for Design Domestic Hot Water HeatingSystem in Ayer Keroh Melaka,Journal of Advanced Research in Fluid Mechanics and Thermal Sciences 56, Issue 1 (2019) 59-67.
[13] Mohamed1, A.M.A.et.al.An investigation into the current utilization and prospective of Renewable Energy Resources and Technologies in Libya.
[14] Cooper, P. I., The absorption of solar radiation in solar stills, Solar Energy 12, 3 (1969).
15].Duffie, J. and Backman, W.2013. 4th edition.Solar engineering of thermal processes. Hoboken New Jersey: John Wiley & Sons, Inc.Subscript n indicates that the radiation is on a plane normal to the Sun-Earth axis.
[16] Fatiha Abdul Rahman(2019), F-Chart Method for Design Domestic Hot Water HeatingSystem in Ayer Keroh Melaka,Journal of Advanced Research in Fluid Mechanics and Thermal Sciences 56, Issue 1 (2019) 59-67.
[16] Liu, B.Y.H. & Jordan, R.C. (1962). Daily insolation on surfaces tilted toward the equator. ASHRAE Transactions, 67, 526-541.
[17] Liu, B.Y.H. & Jordan, R.C. (1960). The interrelationship and characteristic distribution of direct, diffuse, and total solar radiation. Solar Energy, 4(3), 1-19
[18] www.greenrhinoenergy.
